



Universiteit
Leiden
The Netherlands

The effect of PPAR isoform (de)activation on the lipid composition in full-thickness skin models

Helder, R.W.J.; Rousel, J.; Boiten, W.A.; Gooris, G.S.; Nadaban, A.; Ghalbzouri, A. el; Bouwstra, J.A.

Citation

Helder, R. W. J., Rousel, J., Boiten, W. A., Gooris, G. S., Nadaban, A., Ghalbzouri, A. el, & Bouwstra, J. A. (2022). The effect of PPAR isoform (de)activation on the lipid composition in full-thickness skin models. *Experimental Dermatology*, 32(4), 469-478.
doi:10.1111/exd.14733

Version: Publisher's Version

License: [Licensed under Article 25fa Copyright Act/Law \(Amendment Taverne\)](#)

Downloaded from: <https://hdl.handle.net/1887/3514831>

Note: To cite this publication please use the final published version (if applicable).

The effect of PPAR isoform (de)activation on the lipid composition in full-thickness skin models

Richard W. J. Helder¹  | Jannik Rousel¹  | Walter A. Boiten¹  | Gerrit S. Gooris¹ |
 Andreea Nadaban¹  | Abdoelwaheb El Ghalbzouri²  | Joke A. Bouwstra¹

¹Division of Biotherapeutics, LACDR, Leiden University, Leiden, The Netherlands

²Department of Dermatology, LUMC, Leiden, The Netherlands

Correspondence

Joke A. Bouwstra, Division of Biotherapeutics, LACDR, Leiden University, Street: Einsteinweg 55, 2333 CC Leiden, Zuid-Holland, The Netherlands.
 Email: bouwstra@lacdr.leidenuniv.nl

Funding information

Stichting voor de Technische Wetenschappen, Grant/Award Number: 13151

Abstract

Human skin equivalents (HSEs) are 3D-cultured human skin models that mimic many aspects of native human skin (NHS). Although HSEs resemble NHS very closely, the barrier located in the stratum corneum (SC) is impaired. This is caused by an altered lipid composition in the SC of HSEs compared with NHS. One of the most pronounced changes in this lipid composition is a high level of monounsaturations. One key enzyme in this change is stearoyl-CoA desaturase-1 (SCD1), which catalyses the monounsaturations of lipids. In order to normalize the lipid composition, we aimed to target a group of nuclear receptors that are important regulators in the lipid synthesis. This group of receptors are known as the peroxisome proliferating activating receptors (PPARs). By (de)activating each isoform (PPAR- α , PPAR- δ and PPAR- γ), the PPAR isoforms may have normalizing effects on the lipid composition. In addition, another PPAR- α agonist Wy14643 was included as this supplement demonstrated normalizing effects in the lipid composition in a more recent study. After PPAR (ant)agonists supplementation, the mRNA of downstream targets, lipid synthesis genes and lipid composition were investigated. The PPAR downstream targets were activated, indicating that the supplements reached the keratinocytes to trigger their effect. However, minimal impact was observed on the lipid composition after PPAR isoform (de) activation. Only the highest concentration Wy14643 resulted in strong, but negative effects on CER composition. Although the novel tested modifications did not result in an improvement, more insight is gained on the nuclear receptors PPARs and their effects on the lipid barrier in full-thickness skin models.

KEYWORDS

ceramides, monounsaturated, peroxisome proliferating activating receptors, skin, stearoyl-CoA desaturase

Abbreviations: CER, ceramide; FTM, full-thickness models; HSE, human skin equivalent; LPP, long periodicity phase; muCER, monounsaturated ceramide; NHS, native human skin; PPAR, peroxisome proliferating activating receptor; saCER, saturated ceramide; SC, stratum corneum; SCD1, stearoyl-CoA desaturase 1; SPP, short periodicity phase.

© 2022 John Wiley & Sons A/S. Published by John Wiley & Sons Ltd.

1 | INTRODUCTION

Human skin equivalents (HSEs) are *in vitro* cultured skin models designed to mimic the properties of native human skin (NHS) as closely as possible. HSEs are used as a model to study the biological processes in the skin including healthy and disease conditions.¹ In addition, HSEs have another valuable purpose, which is to serve as a prediction model to determine the diffusion profile of novel pharmaceutical compounds across the skin. However, since the barrier of the HSEs is reduced compared with NHS, HSEs cannot be used to their full potential in pharmacokinetics and toxicological screenings.²⁻⁵ Therefore, there is an urgent need for the optimization of the barrier properties in HSEs to better resemble NHS.

The barrier of NHS is located at the stratum corneum (SC), which is the outermost layer of the skin.⁶ This layer consists of two major domains, the corneocytes and the lipid matrix surrounding the corneocytes. Corneocytes are differentiated keratinocytes that contain an envelope of densely cross-linked proteins with a monolayer of lipids, that results in almost impermeable entities.⁶ The lipid matrix in the intercellular space between the corneocytes serves as a continuous permeation pathway through the SC.

The lipid matrix consists of three main lipid classes: cholesterol (CHOL), free fatty acids (FFAs) and ceramides (CERs). In these lipid classes, the most complex classes are FFAs and CERs. FFAs serve as a building block for the even more complex CER subclasses. CERs consist of an acyl chain and a sphingoid base, and currently, in human skin 24 subclasses can be identified. However, in our studies, we used 12 CER subclasses that make up around 97 m/m% of the total amount of CERs.⁸⁻¹¹ More information regarding the various CER subclasses is given in [Figure S1](#).

Together, these lipids form two unique crystalline lamellar phases, referred to as the long periodicity phase (LPP) and the short periodicity phase (SPP) with repeat distances of around 13 nm and 6 nm, respectively.^{12,13} Within the lipid lamellae, the lipids adopt a very dense (orthorhombic), dense (hexagonal) or loose (liquid) packing.^{13,14} This is further explained in [Figure S2](#). In NHS, the lipids adopt predominantly an orthorhombic packing.¹⁵

Although the SC lipid composition of HSEs and NHS has a lot of similarities, several differences are also identified.^{15,16} One of the predominant alterations is an increase in the level of monounsaturated CERs (muCERs). In addition, other important differences were reported such as i) an altered CER subclass profile, ii) an overall reduction in the mean chain length (MCL) of CERs and FFAs,^{17,18} which is also indicated by the increase in the CER with a total chain length of 34 carbons (CER C34) and iii) a reduction in the total amount of FFA compared with the CERs. All together these changes led to the formation of an altered lamellar organization and a reduced lipid packing density. The repeat distance of the LPP is shorter in HSEs than that in NHS and no SPP could be detected in HSEs.¹⁹ Furthermore, most of the lipids form a hexagonal packing rather than a predominantly orthorhombic packing as observed in NHS. Ultimately, these changes in lipid composition and subsequent lipid organization may contribute to a reduced skin barrier.^{17,18,20-23}

In order to improve the lipid composition of HSEs, recent studies demonstrated valuable improvements in HSEs by (down) regulating enzymes or receptors involved in the lipid synthesis.^{16,19} These studies focused on the reduction of a key enzyme that is overexpressed in HSEs, which is stearoyl-CoA desaturase-1 (SCD1).²⁴⁻²⁶ SCD1 was targeted by using a small molecule inhibitor of the enzyme,¹⁹ or by deactivation of the liver X receptor.¹⁶ These studies demonstrated that reducing SCD1 activity has great potential in normalizing the lipid synthesis in HSEs and subsequently improving the lipid organization.

In order to improve the skin barrier of HSE further, in the present study, another family of nuclear receptors is investigated. These are the peroxisome proliferating activating receptors (PPARs), which are involved in the epidermal lipid synthesis pathways.^{27,28} The PPAR family consists of three isoforms, PPAR- α , PPAR- δ and PPAR- γ and are expressed in human skin.^{29,30} PPAR- α and PPAR- γ are mainly expressed in differentiated keratinocytes in the suprabasal epidermis, whereas PPAR- δ is expressed throughout the epidermis.^{31,32} In both murine and human keratinocytes, stimulation of PPAR- α and PPAR- γ increases epidermal differentiation and reduces proliferation.^{33,34} Furthermore, all PPAR isoforms thereby enhance lipid synthesis, formation of lamellar bodies and barrier repair.^{33,35,36} This indicates that PPAR isoforms are interesting candidates for targeting in order to improve the SC lipid composition in HSE and understand the role of the PPARs in the lipid homeostasis. For these studies, we use the in-house HSE, the full-thickness model (FTM).

In this study, the effects of both activation and deactivation on the individual PPARs isoforms were investigated to determine whether (de) activation of a particular isoform has beneficial effects on lipid composition and subsequent lipid organization in FTM.

2 | MATERIALS AND METHODS

The experimental set-up and methods used in this study are briefly described below. A more detailed description and additional techniques, such as cell isolation, SC isolation methods can be found in the [Appendix S1](#).

2.1 | Generation of the full-thickness models

Preparation of the dermal compartment is described in detail in previous studies.^{17,37,38} In each filter insert (Corning Transwell cell culture inserts, membrane diameter 24 mm, pore size 3 μ m; Corning Life Sciences, The Netherlands), 1 ml of a 4 mg/ml collagen solution prepared in acetic acid (0.01% v/v) was used to generate the first layer of collagen. Polymerization of this layer occurred at 37°C for a period of 30 min. Then, a second layer was prepared from 3 ml collagen solution mixed with fibroblasts (4.0 \times 10⁴ cells / ml collagen). This was added on top of the first layer and subsequently polymerized. The dermal compartment was cultured for 7 days as

described previously.^{17,38} After 7 days, 2.5×10^5 keratinocytes were seeded onto each of the dermal compartments and cultured at submerged conditions for a period of 4 days. Subsequently, FTMs were lifted to the air-liquid interface and cultured further for a period of 14–17 days.^{37,39} During this period, various PPAR (ant)agonists, dissolved in dimethyl sulfoxide (DMSO), were supplemented to the culture medium. The PPAR supplements were purchased from Sigma-Aldrich (Zwijndrecht, the Netherlands). The added amount of DMSO was 0.05% v/v of the total amount of medium. In this medium, the following compounds were dissolved to a final concentration as described in Table 1. The agonists, GW7647 (PPAR- α), GW1929 (PPAR- γ) and GW0742 (PPAR- δ) were used in different concentrations, either in $10 \times EC_{50}$ (10x efficacy dose where 50% of the receptor is activated) or $100 \times EC_{50}$ (100x efficacy dose where 50% of the receptor is activated) and the $10 \times IC_{50}$ (inhibition dose where 50% of the receptor is inhibited). The agonist Wy14643 (PPAR- α) was used in two concentrations, the standard $10 \times EC_{50}$ (6.3 μ M) or the concentration used in the recent study (75 μ M).⁴⁰

The $119 \times EC_{50}$ concentration for Wy14643 was chosen as this concentration range has been used in previous studies.^{40,41} The effect of DMSO was included in this study as a control. After analysis, no significant changes were observed in all parameters analysed compared with FTM_{CONTROL} (data not shown). Therefore, FTMs cultured with DMSO were excluded from the results.

All studies were performed in triplicate using keratinocytes and fibroblasts from three different donors (Caucasian female mammae skin donors, aged between 18 and 26). After 14–17 days at the air-liquid interface period, FTMs were harvested and the following analyses were performed: quantitative polymerase chain reaction (qPCR) and liquid chromatography-mass spectrometry (LC-MS) were employed. Only for the PPAR- α Wy14643 agonist samples, Fourier-transformed infrared spectroscopy (FT-IR) and small-angle X-ray diffraction (SAXD) studies were also performed.

TABLE 1 PPAR isoforms supplementation to medium during generation of epidermis of FTMs. The medium concentration of supplementation was either $10 \times EC_{50}$, $100 \times EC_{50}$, $10 \times IC_{50}$ and for Wy14643: $10 \times EC_{50}$ and 75 μ M.

Compound	PPAR isoform	Abbreviation	Effect	EC_{50}/IC_{50} (nM)	$10 \times EC_{50}$	$100 \times EC_{50}$	$10 \times IC_{50}$
GW7647	PPAR- α	FTM- $\alpha_{+(10x)}$	Agonist	6	X		
GW7647	PPAR- α	FTM- $\alpha_{+(100x)}$	Agonist	6		X	
GW6471	PPAR- α	FTM- $\alpha_{-(10x)}$	Antagonist	240			X
GW1929	PPAR- γ	FTM- $\gamma_{+(10x)}$	Agonist	6.2	X		
GW1929	PPAR- γ	FTM- $\gamma_{+(100x)}$	Agonist	6.2		X	
T0070907	PPAR- γ	FTM- $\gamma_{-(10x)}$	Antagonist	1			X
GW0742	PPAR- δ	FTM- $\delta_{+(10x)}$	Agonist	1	X		
GW0742	PPAR- δ	FTM- $\delta_{+(100x)}$	Agonist	1		X	
GSK3787	PPAR- δ	FTM- $\delta_{-(10x)}$	Antagonist	6.6			X
Wy14643	PPAR- α	FTM- $\alpha_{+(Wy 10x)}$	Agonist	630	X		
Wy14643	PPAR- α	FTM- $\alpha_{+(Wy 75 \mu M)}$	Agonist	630		$119 \times (75 \mu M)$	

2.2 | Liquid chromatography-mass spectrometry (LC-MS)

In this study, the CER analysis has been performed according to previously described methods.⁴² In short, complete CER subclass analysis has been performed for the saturated subclasses [NdS], [NS], [NP], [NH], [AdS], [AS], [AP] and [AH] and monounsaturated subclasses muCER [NS] and [AS]. The [EOdS], [EOS], [EOP] and [EOH] subclasses have also been analysed. The ceramide structures are depicted in Figure S1. For the PPAR- α agonist Wy14643 study, CER profile was investigated in more detail. Analysis included all saturated CER[Non-EO] subclasses, all muCER[Non-EO] subclasses and the entire CER[EO] subclasses, including the linoleic/oleic and monounsaturated variants.

2.3 | qPCR analysis

The isolation of the RNA, concentration determination, cDNA synthesis and the run set-up are described in more detail in the supplemental material and methods. In short: the primers designed for this study were as follows: PPAR- α , PPAR- γ , PPAR- δ , CPT1a, CD36, HIPK2, PLIN2, ANGPTL4, ABCA1, SCD1, ELOVL1, ELOVL4, SREBP1c, FAS, ACC, GBA, aSMASE, IVL, FLG and the reference genes SDHA, ZNF410 and ARCP1: (primer sequences are provided in Table S1).

2.4 | Statistical analysis

Statistical analysis was performed using GraphPad 7. A non-paired one-way ANOVA with a Holm-Sidak posttest was used to determine significance between the FTMs and the FTM_{CONTROL}. Significant differences are indicated by * for $p < 0.05$, ** for $p < 0.01$ and *** for $p < 0.001$. NHS from three different donors was compared with the FTM_{CONTROL} with an unpaired T-test.

3 | RESULTS

To examine the effects of (de) activation of the PPAR- α , PPAR- γ and PPAR- δ isoforms in the FTMs, two concentrations of agonist ($10 \times EC_{50}$ and $100 \times EC_{50}$) and one concentration of antagonist ($10 \times IC_{50}$) were supplemented to the culture medium. Two different concentrations of agonist were tested to determine whether the agonist concentration used was sufficient to only activate the selected PPAR isoform as higher concentrations of agonist may contribute to the activation of other members of the PPAR family.

In addition, another series of FTMs that were cultured with PPAR- α agonist referred to as Wy14643. This agonist was chosen because in a previous study this supplement increased the CER content in HSEs.⁴⁰ However, in a more recent study, supplementation of Wy14643 in the medium reduced the CER content in HSE.⁴¹ To determine whether this compound would induce any changes in the CER composition in FTMs, two concentrations of Wy14643 were used. This included $10 \times EC_{50} = 6.3 \mu\text{M}$ (similarly as used in this study for the other PPAR- α , γ and δ supplements) and the highest concentration used in the previous study ($75 \mu\text{M}$ or $119 \times EC_{50}$).

After the culture period, all FTM conditions were viable and samples were harvested to carry out different analyses. RNA was isolated to perform gene expression analysis, and SC was taken for lipid composition analysis via LC-MS and lipid organization studies using FT-IR and SAXD.

3.1 | Successful activation of the PPAR isoform downstream targets of PPAR- α and PPAR- δ

It was important to determine whether the supplements reached the keratinocytes to trigger their effects. To examine this, the FTMs containing the highest concentration of agonist ($100 \times EC_{50}$ for the PPAR isoform supplements and $119 \times EC_{50}$ for Wy14643) were selected to investigate the effect on PPAR downstream targets as well as other lipid synthesis genes of the PPAR isoforms (Figure 1).

First, the PPAR isoform abundances in the skin were examined (Figure 1A). The Ct value presents the amount of material in the sample and can be used as a reference on how much the target primer is present in the sample. Based on the Ct of the PPAR isoforms, an estimation can be made on the abundance of the presence of PPAR isoforms in the skin. All PPAR isoforms are expressed significantly different from each other but PPAR- δ is the most dominant isoform in the FTMs, since the Ct level was the first to reach the threshold, followed by PPAR- α and as last PPAR- γ .

Next, the PPAR downstream targets were studied (Figure 1B). This would indicate whether the PPAR supplements would reach the keratinocytes and trigger an effect. First, PPAR- α downstream target *CPT-1* was investigated. *CPT-1a* was activated by both PPAR- α (GW7647 and Wy14643) and the PPAR- δ supplements in a rather equal amount (~threefold). Second, the PPAR- γ downstream targets *CD36* and *HIPK2* were investigated. However, none of the PPAR supplements induced any changes to the level of these genes. Third, the

PPAR- δ downstream targets *PLIN2* and *ANGPTL4* were investigated. These genes displayed the strongest activation from all the PPAR supplements. *PLIN2* (~threefold) and *ANGPTL4* (~sixfold) were significantly upregulated when targeted by the PPAR- δ supplement. In addition, the PPAR- α agonists GW7647 and Wy14643 also had a significant effect on the downstream target *PLIN2* (~2.5-fold /~threefold, respectively) and *ANGPTL4* (~threefold/~twofold, respectively).

Subsequently, it was investigated whether the PPAR agonists would induce their effect via the nuclear receptor LXR by co-activation, as LXR is also involved in the regulation of *SCD1*. To study this, LXR downstream target *ABCA1* was determined. However, *ABCA1* was only slightly upregulated after supplementation with either PPAR- α Wy14643 or the PPAR- δ agonist (<twofold).

Finally, the lipid synthesis genes, late lipid processing genes and epidermal differentiation genes were investigated (Figure 1C). Minor changes were observed for *FAS* and *ACC*, which were slightly upregulated by PPAR- α agonist Wy14643 (~1.5-fold). Larger differences were observed for the lipid processing genes (Figure 1D). A strong increase in *SCD1* was observed in the FTMs supplemented with the PPAR- δ agonist (~2.5-fold) and an even higher increase for PPAR- α agonist Wy14643 (~threefold). Furthermore, no changes were observed for the lipid elongation enzymes *ELOVL1* and *ELOVL4* between the tested conditions.

3.2 | SC CER composition analysis for the PPAR isoforms

After successful downstream gene target activation of PPAR- α and PPAR- δ , LC-MS analysis of the SC CER composition was performed for all three PPAR isoforms (de) activation, including the Wy14643-treated FTMs.

First, the lipid composition of the CER[non-EO] and CER[EO] subclasses was investigated after (ant)agonist supplementation for PPAR- α : agonist GW7647 + antagonist GW6471 (Figure 2A), PPAR- γ : GW1929 (agonist) + antagonist T0070907 (Figure 2B), PPAR- δ : agonist GW0742 + antagonist GSK3787 (Figure 2C) and PPAR- α : agonist Wy14643 (Figure 2D).

For the $10 \times EC_{50}$ concentration of agonists, all PPAR isoforms displayed a similar CER subclass composition compared with the FTM_{CONTROL} for both CER[non-EO] and CER[EO] subclasses. Even the higher concentration of agonist ($100 \times EC_{50}$) did not result in changes in the CER subclass composition. This was also observed for the FTMs that were supplemented with an antagonist for the deactivation of the PPAR isoforms. Only for the FTM- $\alpha_{+(Wy\ 75\ \mu\text{M})}$, significant effects on the lipid composition were observed (Figure 2D). This included a drastic reduction in the CER[non-EO] subclasses [NH], [AP], [AH] and CER[EO] subclass CER[EOH]. To study the impact of the PPAR- α agonist Wy14643 further, the absolute amounts of the CERs were determined (Figure S3).

It was important to determine whether PPAR- α agonist Wy14643 at varying amounts had an effect on the total CER amount synthesized as this was previously reported.⁴⁰ However, no difference in

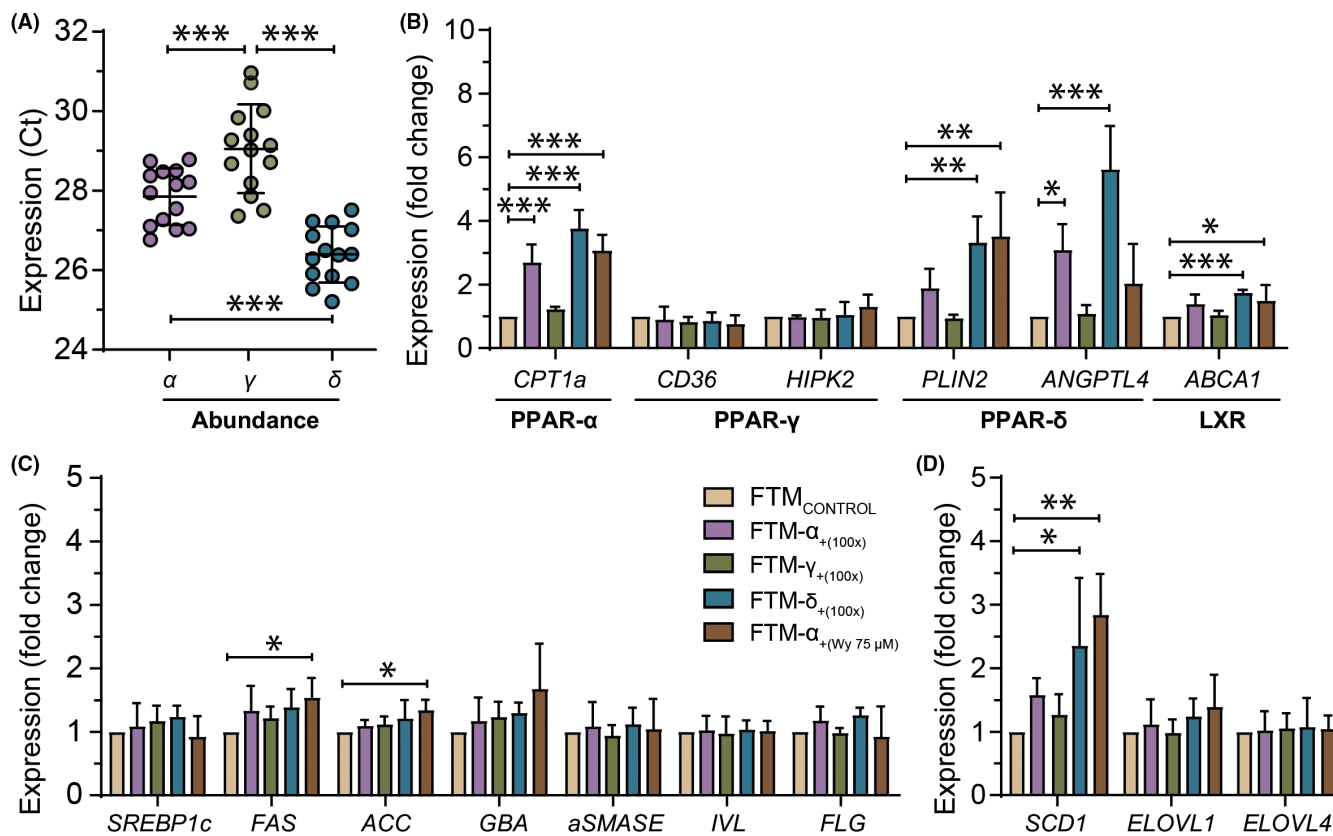


FIGURE 1 Activation of the downstream targets for PPAR- α (GW7647 + Wy14643) and PPAR- δ . qPCR analysis was performed for (A) The expression Ct of PPAR isoforms α , γ and δ (B) PPAR isoform downstream targets and below the nuclear receptor that corresponds to that downstream target (e.g. PPAR- α , PPAR- γ , PPAR- δ or LXR). Furthermore, in (C) the lipid synthesis genes and late lipid processing genes, and (D) lipid processing and lipid differentiation markers. For statistical analysis, a non-paired one-way ANOVA with a Holm-Sidak test was used to determine significance between the FTMs and the FTM_{CONTROL}. Significant differences are indicated by ** for $p < 0.01$ and *** for $p < 0.001$. NHS was compared with the FTM_{CONTROL} with an unpaired T -test.

the amount of total CERs was observed between all tested conditions (Figure S3A). For the CER[non-EO] and CER[EO] subclasses, a similar trend was observed. However, due to the higher error bars when dealing with absolute values, these changes were not significant.

Finally, NHS was compared with the FTM. NHS displayed differences in the CER profile compared with the FTM_{CONTROL} for CER [NS], [NP], [NH], [AS], [AP] and [EOS] similarly as reported previously.^{15,16,38}

Next, for all the PPAR isoforms, the MCL and degree of mono-unsaturation were investigated. The mono-unsaturation percentage was calculated for CER [NS] and [AS], and the muCER% is defined as $(\text{muCER [NS+AS]} / (\text{muCER [NS+AS]} + \text{saCER [NS+AS]})) * 100$. Similar percentages of the muCER% of CER [NS] + [AS] were observed for all tested conditions (Figure 2E) except for FTM- $\alpha_{+(75 \mu\text{M})}$, in which the muCERs were significantly increased. In addition, the absolute amount of muCER was also increased for FTM- $\alpha_{+(75 \mu\text{M})}$ (Figure S3D). The fraction of muCERs in all FTMs was much higher than in the SC of NHS. Furthermore, no differences in the lipid chain length for the MCL of CER[non-EO] and CER[EO] (Figure 2F,G, respectively) were observed in the FTMs either except for the strong reduction in MCL of both CER[non-EO] and

CER[EO] in the FTM- $\alpha_{+(75 \mu\text{M})}$. Compared with FTMs, NHS had a much higher MCL for CER[non-EO]. Finally, to determine whether there was an effect on the overall lipid chain length distribution, the percentage of CER C34 was investigated (Figure 2H). A small trend was observed for the fraction of CER C34 in the PPAR (ant)agonist-treated conditions, which were slightly higher compared with the FTM_{CONTROL}, but this was not significant. Only the percentage of CER C34 was increased in the FTM- $\alpha_{+(75 \mu\text{M})}$.

For comparison, the percentage of CER C34 is very low in NHS.

3.3 | Lipid organization after PPAR- α Wy14643 activation

As there were significant changes in the lipid composition of the FTM- $\alpha_{+(75 \mu\text{M})}$, it is of interest to determine the effects on the lipid organization.

From the CH_2 rocking vibration region in the infrared spectrum, the lateral organization can be determined (Figure 3A). At 0°C, the highest intensity peak is present at 719 cm^{-1} and a smaller peak is present at 730 cm^{-1} in the spectrum of the FTM_{CONTROL}. This indicates that the lipids in the SC predominantly adopt a hexagonal

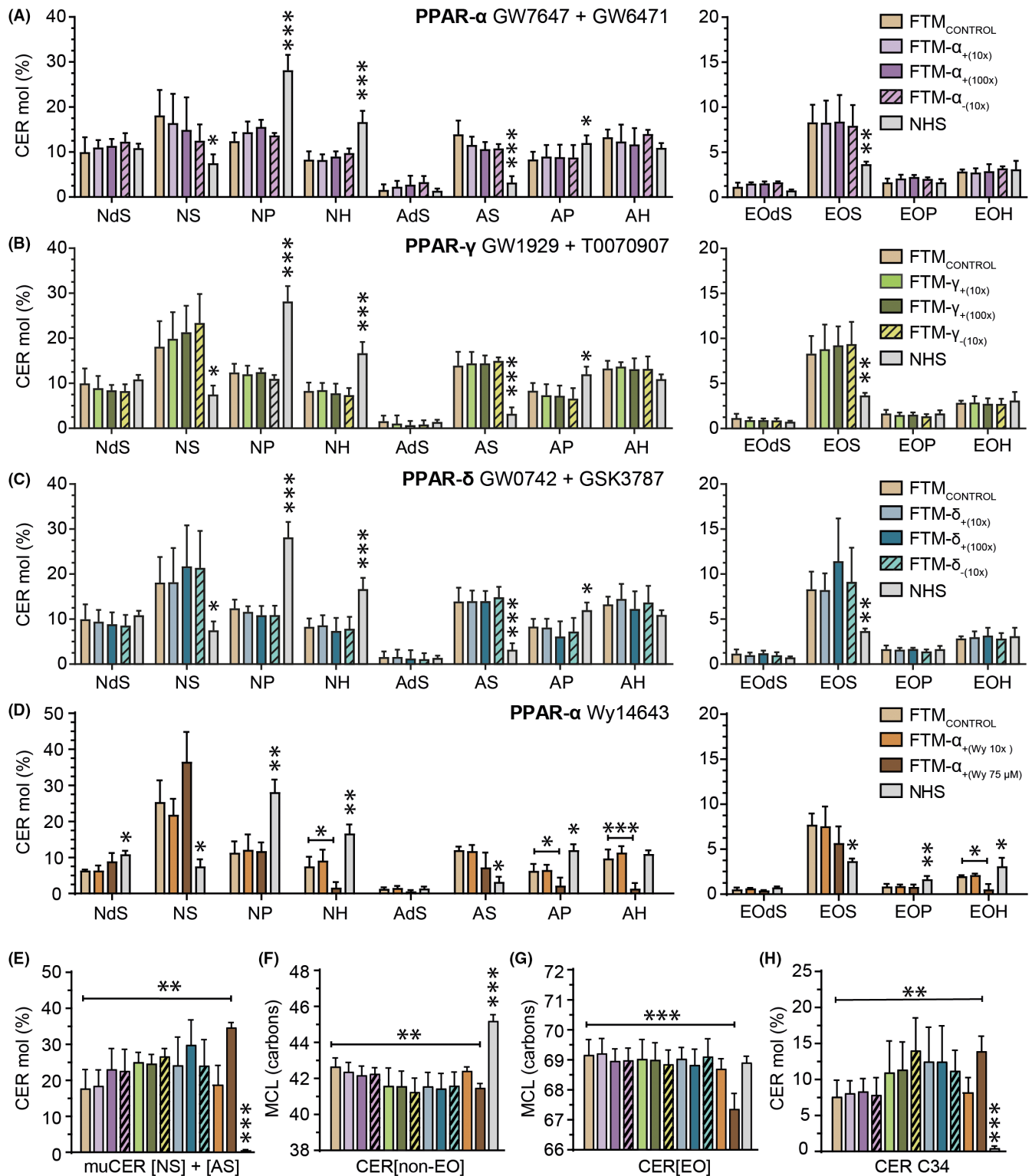


FIGURE 2 PPAR isoform (de) activation led to a similar lipid composition except for PPAR- α Wy14643, which displayed significant changes in the lipid composition. The saturated CER[non-EO] and saturated CER[EO] subclasses are plotted for all PPAR isoforms with their corresponding (ant)agonist (A) PPAR- α GW7647 (agonist) + GW6471 (antagonist), (B) PPAR- γ GW1929 (agonist) + T0070907 (antagonist), (C) PPAR- δ GW0742 (agonist) + GSK3787 (antagonist), (D) PPAR- α Wy14643 (agonist). In addition, lipid processing was examined for: (E) muCERs, (F) MCL of the saturated CER[non-EO], (G) MCL of the saturated CER[EO] subclasses and (H) CER C34%. For statistical analysis, a non-paired one-way ANOVA with a Holm-Sidak test was used to determine significance between the FTMs and the FTM_{CONTROL}. Significant differences are indicated by * for $p < 0.05$, ** for $p < 0.01$ and *** for $p < 0.001$. NHS was compared with the FTM_{CONTROL} with an unpaired T-test.

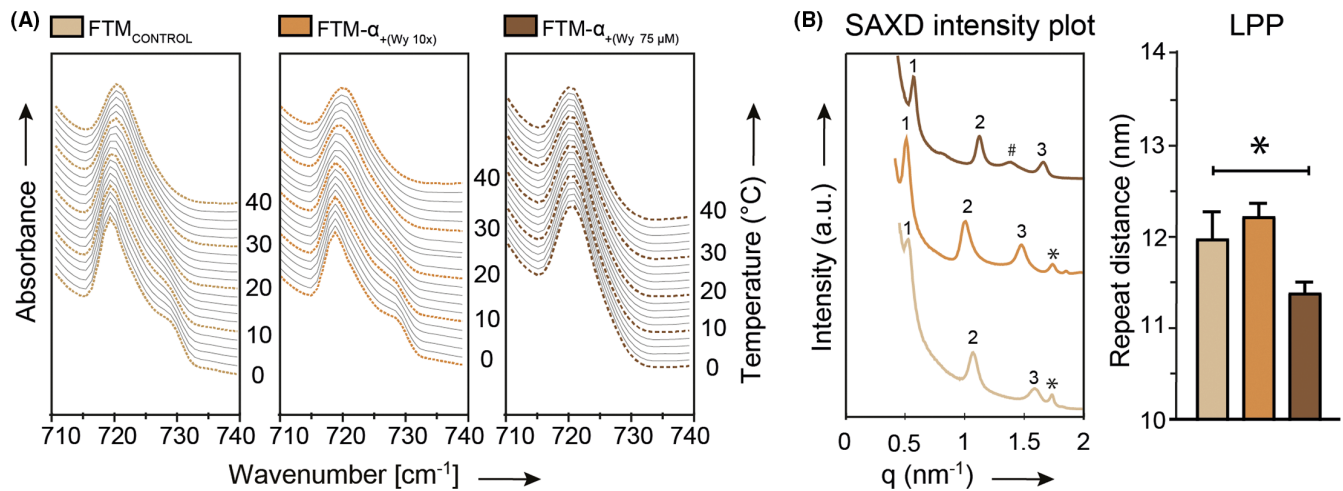


FIGURE 3 PPAR- α agonist Wy14643 enhances the fraction of lipids forming a hexagonal packing and significantly reduced the LPP repeat distance. The lipid organization was determined. The lateral organization was monitored by measuring the (A) rocking vibrations of the lipid chains in the infrared spectrum from 0 to 40°C; (B) the lamellar organization was determined from the X-ray diffraction profile of the FTM_{CONTROL}, FTM- $\alpha_{\text{Wy}10x}$ and FTM- $\alpha_{\text{Wy}75\mu\text{M}}$ and is shown in arbitrary units (a.u.). From these peaks, the 1st, 2nd, and 3rd order diffraction peak attributed to the LPP are indicated as Arabic numerals. Cholesterol is indicated as *. In addition, another unknown phase is detected and indicated as #. A non-paired one-way ANOVA with a Holm-Sidak test was used to determine significance between the FTMs and the FTM_{CONTROL}. Significant differences are indicated by * for $p < 0.05$

packing, but there is a small fraction of lipids forming the orthorhombic packing. No difference is observed between the FTM_{CONTROL} and the FTM- $\alpha_{\text{Wy}10x}$. However, the FTM- $\alpha_{\text{Wy}75\mu\text{M}}$ displays no peak at 730 cm⁻¹, indicating that the lipid fraction adopts a hexagonal packing and the orthorhombic packing is not detectable. Next, the lamellar lipid organization was determined (Figure 3B). The FTM- $\alpha_{\text{Wy}10x}$ and the FTM_{CONTROL} had a similar LPP repeat distance. In case of FTM- $\alpha_{\text{Wy}75\mu\text{M}}$ there is an additional peak indicated by “#” in the spectrum, which is probably attributed by the change in lipid composition. In addition, when comparing the FTM- $\alpha_{\text{Wy}75\mu\text{M}}$ to the FTM_{CONTROL} diffraction curve, a significant reduction in the repeat distance of the LPP was observed, while phase-separated cholesterol disappeared.

4 | DISCUSSION

The involvement of PPARs in epidermal lipid synthesis and homeostasis has been documented in several studies.^{32,35,43} Since many of the used compounds at high concentration trigger multiple PPAR isoforms, the goal of this study was to capture the individual effects of the PPAR isoform on the lipid properties of FTM. To this end, a concentration of $10 \times \text{EC}_{50}$ / IC_{50} was selected for the (ant)agonists to prevent another PPAR isoform from (de)activation. In addition, for the agonists, it was decided to include an additional concentration of $100 \times \text{EC}_{50}$, as this allowed us to study the effect of agonists at a rather high concentration of medium supplementation and still be able to monitor whether other PPAR isoforms are affected. The targeted approach for individual PPAR isoforms combined with a state-of-the-art LC-MS analysis allows us to analyse the CER composition not only to distinguish between the effects on the CER subclass

composition but also on the effects of lipid chain length and degree of monounsaturations of CERs.

After supplementing the culture medium with the PPAR agonist concentration ($100 \times \text{EC}_{50}$) during the development of FTMs, effects on the downstream targets were observed on mRNA levels for PPAR- α (GW7647 and Wy14643) and PPAR- δ (GW0742). Therefore, it can be concluded that both PPAR- δ and PPAR- α supplements reached the keratinocytes. Unfortunately, the downstream targets of PPAR- γ supplement (GW1929) were unaffected, so for this agonist it remains uncertain whether the agonist was able to reach the keratinocytes. However, as PPAR- γ targeted FTM had the lowest Ct value of the PPAR isoforms, it might be that the amount of receptor present is too low to trigger an adequate response.

Although both PPAR- α and PPAR- δ agonists had similar effects on the downstream targets, they did not result in a similar lipid composition. The 75 μM supplementation of PPAR- α agonist Wy14643 activated SCD1 in the FTM to a much greater extent than the PPAR- α agonist GW7647 or PPAR- δ agonist GW0742. This increased SCD1 expression might explain the difference in the muCER content. Yet, it remains unknown what drives these changes in the CER profile. However, it is important to note that this difference in effect is likely not caused by LXR activation, as both compounds activate ACBA1 to the same extent.

Previous studies in mice and HSEs reported beneficial changes by activating the PPAR isoforms after barrier disruption.^{36,40,44,45} In these studies, PPAR activation after barrier disruption resulted in an enhancing effect towards barrier recovery, such as increased lipid metabolism,^{36,41,46} increased differentiation, reduced proliferation,^{34,41,47} and barrier recovery.⁴⁸ However, these effects were not found in our studies. There might be at least three possible explanations: (1) it is possible that the activation of the downstream targets

in the present study was not sufficient to trigger the subsequent effects on the lipid synthesis in our FTMs. However, the downstream genes were activated, but perhaps a higher concentration is required to create a significant effect on CER profiles. (2) In the studies that were performed in vivo (murine), PPAR agonists were applied on the skin surface after barrier disruption. The barrier disruption itself will trigger a quicker SC regeneration, and the supplements are applied locally. This might lead to higher local concentrations of the PPARs in the epidermis then when PPARs are supplemented in culture medium at a constant concentration over a longer time period. This creates a different scenario that might have an impact. (3) Possibly PPAR (ant)agonists trigger indirect effects when in vivo models are used. For example, studies performed in vivo (murine) might trigger an immune response. PPARs are known for their anti-inflammatory properties through suppressing pro-inflammatory cytokines, chemokines and Toll-like receptors.^{49–53} Both PPAR- α and PPAR- γ are known to promote a regulatory T-cell response suppressing the immune response.^{54,55} This could be an important effect of the PPARs in vivo, as it is known that pro-inflammatory cytokines can affect keratinocytes quite substantial. In a recent study of Danso et al, it was demonstrated that the pro-inflammatory cytokine TNF- α negatively impacted the CER and FFA composition.⁵⁶

Although the effects of the three PPAR isoforms supplements did not result in changes in lipid composition, the PPAR- α agonist Wy14643 supplementation at very high concentration led to unfavourable changes in CER composition. The most pronounced effects were as follows: (i) An increase in muCERs[non-EO] that was accompanied by a significant increase in *SCD1* on mRNA level. (ii) Significant reduction in hydrophilic CER subclasses, especially of CER[H] subclasses, in both CER[non-EO] and CER[EO]. (iii) A reduction in the MCL of both saCERs[non-EO] and saCERs[EO]. These changes led to a reduced packing density (lateral lipid organization) and a reduced repeat distance of the LPP.

There are some inconsistencies between studies performed with PPAR- α agonist Wy14643 supplementation in HSEs. In the study performed by Rivier et al (2015), the addition of Wy14643 enhanced CER synthesis,⁴⁰ whereas another study performed by Wallmeyer et al (2015) reported a decrease in CER amounts after the supplementation of Wy14643.⁴¹ In our study, there is no change in the total amount of CERs, but a drastic change in the CER composition: the most hydrophilic CERs reduced significantly after supplementation of Wy14643. In the two previous studies, no Vitamin C was supplemented to the medium. As a consequence, the synthesis of the most hydrophilic CER subclasses in these studies was already reduced, which of course affects the outcome of the studies.³⁹

As observed in PPAR- α -deficient mice, lipogenic genes such as *FAS*, *SREBP1c* and *SCD1* were completely abolished.⁵⁷ Therefore, a possible explanation for the strong effect of PPAR- α on the lipid composition is the stimulation of *SCD1*. Our results are in agreement with these findings: a high concentration of Wy14643 causes the increase in these genes. However, the subsequent effects, such as the reduction in MCL as well as the reduction in the more hydrophilic CER subclasses CER [NH], [AdS], [AS], [AP] and [H] subclasses,

are not fully understood. However, based on our results, the supplementation of Wy14643 seems to indicate that this pathway has been severely affected. Another interesting observation was that the CER amount was not affected by Wy14643. This was also observed in previous studies, in which the effect of supplementation of the *SCD1* inhibitor or a deactivator of LXR on CER composition was examined.^{16,19} This indicates that the specific CER subclass profile synthesis is changed during FTM development, but it does not affect the amount of CERs synthesized.

To conclude, this study demonstrated the complexity of the lipid synthesis pathways and that the effects of the PPAR isoforms. However, the changes in lipid composition and subsequent organization were not beneficial for the FTM, but in the case of Wy14643 supplementation, these changes are detrimental for the subsequent SC lipid properties and are contrasting with previous studies.^{16,20,23} Although the novel tested methods in this study did not directly improve our in-house FTM model, more insight is gained of the nuclear receptors PPARs and their effects in 3D-skin tissue engineering.

AUTHOR CONTRIBUTIONS

Author Contributions: RWJH, JAB and AEG designed the research study. RWJH, JR, WAB, AN and GSG performed the research. RWJH, JR, WAB and AN performed the data analysis. RWJH drafted the manuscript, which was commented on by JAB and AEG. All authors approved the submitted manuscript.

ACKNOWLEDGEMENTS

We would like to thank the DUBBLE beamline BM26 staff at the European synchrotron radiation facility (Grenoble, France) for their support and the company Evonik for their supply of ceramides.

FUNDING INFORMATION

This research was supported by the Dutch Technology Foundation STW (Grant 13151) and is part of the Netherlands Organization for Scientific Research (NWO).

CONFLICT OF INTEREST

The authors declare no conflicts of interest.

DATA AVAILABILITY STATEMENT

The data that support the findings of this study are available from the corresponding author upon reasonable request.

INSTITUTIONAL REVIEW BOARD STATEMENT

During the experiments, the Declaration of Helsinki principles were followed during obtainment of primary cells from human skin originating from surplus breast tissue of healthy female donors (between age 18–45). The experiments conducted in this study were in accordance with article 7:467 of the Dutch Law on Medical Treatment Agreement and the Code for proper Use of Human Tissue of the Dutch Federation of Biomedical Scientific Societies (<https://www.federa.org/codes-conduct>). As of this national legislation, coded surplus tissue can be used for scientific research purposes when

no written objection is made by the informed donor. Therefore, additional approval of an ethics committee regarding scientific use of surplus tissue was not obligatory.


ORCID

Richard W. J. Helder  <https://orcid.org/0000-0002-5681-4471>

Jannik Rousel  <https://orcid.org/0000-0003-0986-3753>

Walter A. Boiten  <https://orcid.org/0000-0001-9060-6222>

Andreea Nadaban  <https://orcid.org/0000-0002-4981-6268>

Abdoelwaheb El Ghalbzouri  <https://orcid.org/0000-0001-8351-7715>

REFERENCES

- Lilienblum W, Dekant W, Foth H, et al. Alternative methods to safety studies in experimental animals: role in the risk assessment of chemicals under the new European chemicals legislation (REACH). *Arch Toxicol*. 2008;82(4):211-236. doi:10.1007/s00204-008-0279-9
- Schäfer-Korting M, Bock U, Gamer A, et al. Reconstructed human epidermis for skin absorption testing: results of the German prevalence study. *Altern Lab Anim*. 2006;34(3):283-294.
- Van Gele M, Geusens B, Brochez L, Speeckaert R, Lambert J. Three-dimensional skin models as tools for transdermal drug delivery: challenges and limitations. *Expert Opin Drug Deliv*. 2011;8(6):705-720.
- Flaten GE, Palac Z, Engesland A, Filipović-Grčić J, Vanić Z, Škalko-Basnet N. In vitro skin models as a tool in optimization of drug formulation. *Eur J Pharm Sci*. 2015;30(75):10-24. doi:10.1016/j.ejps.2015.02.018
- Planz V, Lehr C-M, Windbergs M. In vitro models for evaluating safety and efficacy of novel technologies for skin drug delivery. *J Control Release*. 2016;242:89-104. doi:10.1016/j.jconrel.2016.09.002
- Proksch E, Brandner JM, Jensen J-M. The skin: an indispensable barrier. *Exp Dermatol*. 2008;17(12):1063-1072. doi:10.1111/j.1600-0625.2008.00786.x
- Masukawa Y, Narita H, Sato H, Naoe A, Kondo N, Sugai Y. Comprehensive quantification of ceramide species in human stratum corneum. *J Lipid Res*. 2009;50(8):1708-1719. doi:10.1194/jlr.D800055-JLR200
- Rabionet M, Gorgas K, Sandhoff R. Ceramide synthesis in the epidermis. *Biochim Biophys Acta*. 2014;1841(3):422-434. doi:10.1016/j.bbaliip.2013.08.011
- van Smeden J, Hoppel L, van der Heijden R, Hankemeier T, Vreeken RJ, Bouwstra JA. LC/MS analysis of stratum corneum lipids: ceramide profiling and discovery. *J Lipid Res*. 2011;52(6):1211-1221. doi:10.1194/jlr.M014456
- t'Kindt J, Jorge L, Dumont E, et al. Profiling and characterizing skin ceramides using reversed-phase liquid chromatography-quadrupole time-of-flight mass spectrometry. *Anal Chem*. 2012;84(1):403-411. doi:10.1021/ac202646v
- Miyamoto M, Kawana M, Ohno Y, Kihar A. Comparative profiling and comprehensive quantification of stratum corneum ceramides in humans and mice by LC/MS/MS. *J Lipid Res*. 2020;61(6):884-895. doi:10.1194/jlr.RA120000671
- Bouwstra JA, Gooris GS, van der Spek JA, Bras W. Structural investigations of human stratum corneum by small-angle X-ray scattering. *J Invest Dermatol*. 1991;97(6):1005-1012. doi:10.1111/1523-1747.ep12492217
- Boncheva M. The physical chemistry of the stratum corneum lipids. *Int J Cosmet Sci*. 2014;36(6):505-515. doi:10.1111/ics.12162
- Bouwstra JA, Gooris GS. The lipid organisation in human stratum corneum and model systems. *The Open Dermatology Journal*. 2010;4(1):10-13. doi:10.2174/1874372201004010010
- Mieremet A, Helder RWJ, Boiten WA, et al. Contribution of palmitic acid to epidermal morphogenesis and lipid barrier formation in human skin equivalents. *Int J Mol Sci*. 2019;20(23):6069. doi:10.3390/ijms20236069
- Helder RWJ, Boiten W, van Dijk R, Gooris G, El Ghalbzouri A, Bouwstra J. The effects of LXR agonist T0901317 and LXR antagonist GSK2033 on morphogenesis and lipid properties in full thickness skin models. *Biochim Biophys Acta Mol Cell Biol Lipids*. 2020;1865(2):158546. doi:10.1016/j.bbaliip.2019.158546
- Thakoersing VS, Gooris GS, Mulder AA, Rietveld M, El Ghalbzouri A, Bouwstra JA. Unraveling barrier properties of three different in-house human skin equivalents. *Tissue Eng Part C Methods*. 2012;18(1):1-11. doi:10.1089/ten.TEC.2011.0175
- Thakoersing VS, van Smeden J, Mulder AA, Vreeken RJ, El Ghalbzouri A, Bouwstra JA. Increased presence of monounsaturated fatty acids in the stratum Corneum of human skin equivalents. *J Invest Dermatol*. 2013;133(1):59-67. doi:10.1038/jid.2012.262
- Helder RWJ, Rousel J, Boiten WA, et al. Improved organotypic skin model with reduced quantity of monounsaturated ceramides by inhibiting stearoyl-CoA desaturase-1. *Biochimica et Biophysica Acta (BBA) - molecular and cell biology of Lipids*. 2021;1866(4):158885. doi:10.1016/j.bbaliip.2021.158885
- Mojumdar EH, Helder RWJ, Gooris GS, Bouwstra JA. Monounsaturated fatty acids reduce the barrier of stratum Corneum lipid membranes by enhancing the formation of a hexagonal lateral packing. *Langmuir* 2014/06/10 2014;30(22):6534-6543. doi:10.1021/la500972w
- van Smeden J, Janssens M, Kaye EC, et al. The importance of free fatty acid chain length for the skin barrier function in atopic eczema patients. *Exp Dermatol*. 2014;23(1):45-52. doi:10.1111/exd.12293
- Ishikawa J, Narita H, Kondo N, et al. Changes in the Ceramide Profile of Atopic Dermatitis Patients. *J Invest Dermatol*. 2010;130(10):2511-2514. doi:10.1038/jid.2010.161
- van Smeden J, Bouwstra JA. Stratum Corneum lipids: their role for the skin barrier function in healthy subjects and atopic dermatitis patients. *Curr Probl Dermatol*. 2016;49:8-26. doi:10.1159/000441540
- Paton CM, Ntambi JM. Biochemical and physiological function of stearoyl-CoA desaturase. *Am J Physiol Endocrinol Metab*. 2009;297(1):E28-E37. doi:10.1152/ajpendo.90897.2008
- Schultz JR, Tu H, Luk A, et al. Role of LXRs in control of lipogenesis. *Genes Dev*. 2000;14:2831-2838. doi:10.1101/gad.850400
- Thakoersing VS, van Smeden J, Boiten WA, et al. Modulation of stratum corneum lipid composition and organization of human skin equivalents by specific medium supplements. *Exp Dermatol*. 2015;24(9):669-674. doi:10.1111/exd.12740
- Kersten S, Desvergne B, Wahli W. Roles of PPARs in health and disease. *Nature*. 2000;405(6785):421-424. doi:10.1038/35013000
- Willson TM, Brown PJ, Sternbach DD, Henke BR. The PPARs: from orphan receptors to drug discovery. *J Med Chem*. 2000;43(4):527-550. doi:10.1021/jm990554g
- Westergaard M, Henningsen J, Svendsen ML, et al. Modulation of keratinocyte gene expression and differentiation by PPAR-selective ligands and tetradecylthioacetic acid. *J Invest Dermatol*. 2001;116:702-712. doi:10.1046/j.1523-1747.2001.01329.x
- Matsuura H, Adachi H, Smart RC, Xu X, Arata J, Jetten AM. Correlation between expression of peroxisome proliferator-activated receptor beta and squamous differentiation in epidermal and tracheobronchial epithelial cells. *Mol Cell Endocrinol*. 1999;147:85-92.
- Icre G, Wahli W, Michalik L. Functions of the peroxisome proliferator-activated receptor (PPAR) alpha and beta in skin homeostasis, epithelial repair, and morphogenesis. *J Invest Dermatol Symp Proc*. 2006;11(1):30-35. doi:10.1038/sj.jidsymp.5650007

32. Rivier M, Safonova I, Lebrun P, Griffiths CE, Ailhaud G, Michel S. Differential expression of peroxisome proliferator-activated receptor subtypes during the differentiation of human keratinocytes. *J Invest Dermatol*. 1998;111(6):1116-1121.
33. Kim DJ, Murray IA, Burns AM, Gonzalez FJ, Perdew GH, Peters JM. Peroxisome proliferator-activated receptor-beta/delta inhibits epidermal cell proliferation by down-regulation of kinase activity. *J Biol Chem*. 2005;280:9519-9527.
34. Yang Q, Yamada A, Kimura S, Peters JM, Gonzalez FJ. Alterations in skin and stratified epithelia by constitutively activated PPARalpha. *J Invest Dermatol*. 2006;126(2):374-385. doi:10.1038/sj.jid.5700056
35. Schmutz M, Moosbrugger-Martinez V, Blunder S, Dubrac S. Role of PPAR, LXR, and PXR in epidermal homeostasis and inflammation. *Biochim Biophys Acta*. 2014;1841(3):463-473. doi:10.1016/j.bbali.2013.11.012
36. Man M, Choi E, Schmutz M, et al. Basis for improved permeability barrier homeostasis induced by PPAR and LXR activators: liposensors stimulate lipid synthesis, lamellar body secretion, and post-secretory lipid processing. *J Invest Dermatol*. 2006;126(2):386-392. doi:10.1038/sj.jid.5700046
37. van Drongelen V, Danso MO, Mulder A, et al. Barrier properties of an N/TERT-based human skin equivalent. *Tissue Eng Part A*. 2014;20(21-22):3041-3049. doi:10.1089/ten.TEA.2014.0011
38. Mieremet A, Rietveld M, Absalah S, Van Smeden J, Bouwstra JA, El Ghalbzouri A. Improved epidermal barrier formation in human skin models by chitosan modulated dermal matrices. *PLoS One*. 2017;12(3):e0174478. doi:10.1371/journal.pone.0174478
39. Ponc M, Weerheim A, Kempenaar J, et al. The formation of competent barrier lipids in reconstructed human epidermis requires the presence of vitamin C. *J Invest Dermatol*. 1997;109(3):348-355. doi:10.1111/1523-1747.ep12336024
40. Rivier M, Castiel I, Safonova I, Ailhaud G, Michel S. Peroxisome proliferator-activated receptor-alpha enhances lipid metabolism in a skin equivalent model. *J Invest Dermatol*. 2000;114(4):681-687. doi:10.1046/j.1523-1747.2000.00939.x
41. Wallmeyer L, Lehnen D, Eger N, et al. Stimulation of PPAR α normalizes the skin lipid ratio and improves the skin barrier of normal and filaggrin deficient reconstructed skin. *J Dermatol Sci*. 2015;80(2):102-110. doi:10.1016/j.jdermsci.2015.09.012
42. Boiten WA, Absalah S, Vreeken RJ, Bouwstra JA, van Smeden J. Quantitative analysis of ceramides using a novel lipidomics approach with three dimensional response modelling. *Biochim Biophys Acta*. 2016;1861(11):1652-1661. doi:10.1016/j.bbali.2016.07.004
43. Schmutz M, Haq CM, Cairns WJ, et al. Peroxisome proliferator-activated receptor (PPAR)- β/δ stimulates differentiation and lipid accumulation in keratinocytes. *J Invest Dermatol*. 2004;122:971-983. doi:10.1111/j.0022-202X.2004.22412.x
44. Rakhshandehroo M, Hooiveld G, Müller M, Kersten S. Comparative analysis of gene regulation by the transcription factor PPAR α between mouse and human. *PLoS One*. 2009;4(8):e6796. doi:10.1371/journal.pone.0006796
45. Heikkinen S, Auwerx J, Argmann CA. PPARgamma in human and mouse physiology. *Biochim Biophys Acta*. 2007;1771(8):999-1013. doi:10.1016/j.bbali.2007.03.006
46. Rivier M, Castiel I, Safonova I, Ailhaud G, Michel S. Peroxisome proliferator-activated receptor- α enhances lipid metabolism in a skin equivalent model. *J Invest Dermatol*. 2000;114(4):681-687. doi:10.1046/j.1523-1747.2000.00939.x
47. Tan NS, Michalik L, Noy N, et al. Critical roles of PPAR beta/delta in keratinocyte response to inflammation. *Genes Dev*. 2001;15(24):3263-3277. doi:10.1101/gad.207501
48. Lim SW, Hong SP, Jeong SW, et al. Simultaneous effect of ursolic acid and oleanolic acid on epidermal permeability barrier function and epidermal keratinocyte differentiation via peroxisome proliferator-activated receptor-alpha. *J Dermatol*. 2007;34(9):625-634. doi:10.1111/j.1346-8138.2007.00344.x
49. Dubrac S, Stoitzner P, Pirkebner D, et al. Peroxisome proliferator-activated receptor-alpha activation inhibits Langerhans cell function. *J Immunol*. 2007;178(7):4362-4372. doi:10.4049/jimmunol.178.7.4362
50. Dubrac S, Schmutz M. PPAR-alpha in cutaneous inflammation. *Dermatoendocrinol*. 2011;3(1):23-26. doi:10.4161/derm.3.1.14615
51. Chong HC, Tan MJ, Philippe V, et al. Regulation of epithelial-mesenchymal IL-1 signaling by PPARbeta/delta is essential for skin homeostasis and wound healing. *J Cell Biol*. 2009;184(6):817-831. doi:10.1083/jcb.200809028
52. Aarenstrup L, Flindt EN, Otkjaer K, Kirkegaard M, Andersen JS, Kristiansen K. HDAC activity is required for p65/RelA-dependent repression of PPARdelta-mediated transactivation in human keratinocytes. *J Invest Dermatol*. 2008;128(5):1095-1106. doi:10.1038/sj.jid.5701146
53. Dasu MR, Park S, Devaraj S, Jialal I. Pioglitazone inhibits toll-like receptor expression and activity in human monocytes and db/db mice. *Endocrinology*. 2009;150(8):3457-3464. doi:10.1210/en.2008-1757
54. Lei J, Hasegawa H, Matsumoto T, Yasukawa M. Peroxisome proliferator-activated receptor α and γ agonists together with TGF- β convert human CD4+CD25- T cells into functional Foxp3+ regulatory T cells. *J Immunol*. 2010;185(12):7186-7198. doi:10.4049/jimmunol.1001437
55. Wohlfert EA, Nichols FC, Nevisus E, Clark RB. Peroxisome proliferator-activated receptor gamma (PPARgamma) and immunoregulation: enhancement of regulatory T cells through PPARgamma-dependent and -independent mechanisms. *J Immunol*. 2007;178(7):4129-4135. doi:10.4049/jimmunol.178.7.4129
56. Danso MO, van Drongelen V, Mulder A, et al. TNF- α and Th2 cytokines induce atopic dermatitis-like features on epidermal differentiation proteins and stratum corneum lipids in human skin equivalents. *J Invest Dermatol*. 2014;134(7):1941-1950. doi:10.1038/jid.2014.83
57. Hebbachi AM, Knight BL, Wiggins D, Patel DD, Gibbons GF. Peroxisome proliferator-activated receptor α deficiency abolishes the response of Lipogenic gene expression to Re-feeding: restoration of the normal response by activation of liver x receptor α . *J Biol Chem*. 2008;283(8):4866-4876. doi:10.1074/jbc.M709471200

SUPPORTING INFORMATION

Additional supporting information can be found online in the Supporting Information section at the end of this article.

Figure S1.

Figure S2.

Figure S3.

Table S1.

Appendix S1.

How to cite this article: Helder RWJ, Rousel J, Boiten WA, et al. The effect of PPAR isoform (de)activation on the lipid composition in full-thickness skin models. *Exp Dermatol*. 2023;32:469-478. doi:10.1111/exd.14733